Supporting Information for

Near-Infrared Electron Acceptors Based on Terrylene Diimides for Organic Solar Cells

Ningning Liang,[a] Kai Sun,[b] Jiajing Feng,[a] Yu Chen,[c] Dong Meng,[c] Wei Jiang,[c] Yan Li,[c] Jianhui Hou,[*,c] Zhaohui Wang[*,a]

[a] Key Laboratory of Organic Optoelectronics and Molecular Engineering, Department of Chemistry, Tsinghua University, Beijing, 100084, P. R. China

[b] State Key Laboratory of PV Science and Technology, Changzhou, 213000, P. R. China.

[c] Institute of Chemistry, Chinese Academy of Sciences, Beijing, 100190, P. R. China

Table of Contents

1. Materials and Characterization Techniques

^{1}H nuclear magnetic resonance (NMR) and ^{13}C NMR spectra were recorded in deuterated solvents on a Bruker AVIII 500WB NMR spectrometer. NMR chemical shifts are reported in parts per million downfield from a tetramethylsilane (TMS) reference using the residual protonated solvent as an internal standard. HR-MALDI-TOF mass spectra were determined on Bruker solariX 9.4 Tesla Fourier Transform Mass Spectrometer. Ultraviolet−visible (UV−vis) absorption spectra were measured with a Hitachi (Model U-3010) spectrophotometer in a 1-cm quartz cell. Cyclic voltammograms (CV) were recorded on a Zahner IM6e electrochemical workstation using glassy carbon discs as the working electrode, Pt wire as the counter electrode, Ag/AgCl electrode as the reference electrode at a scanning rate of 100 mV/s. 0.1 M Bu_4NPF_6 (tetrabutylammoniumhexafluorophosphate) was dissolved in acetonitrile, which was calibrated by the ferrocene/ferroncenium (Fc/Fc^+) as the redox couple. The thin films were deposited from $CHCl_3$ solution onto the working electrode. All chemicals were purchased from commercial suppliers and used without further purification unless otherwise specified.

TDI: 1H NMR (500 MHz, CDCl2CDCl2, 373K): δ = 8.61-8.60 (d, J = 8.0 Hz, 4H), 8.50 (s, 4H), 8.45-8.44 (d, J = 8.0 Hz, 4H), 5.22-5.16 (m, 2H), 2.29-2.24 (m, 4H), 1.98-1.92 (m, 4H), 1.42-1.33 (m, 24H), 0.90-0.87 (m, 12H); 13C NMR (125 MHz, CDCl2CDCl2, 373K): δ = 164.15, 135.44, 131.32, 131.11, 129.82, 128.78, 126.10, 124.15, 122.58, 121.37, 54.83, 32.61, 31.74, 26.68, 22.45, 13.84; HRMS (MALDI, 100%): calcd (%) for C56H58N2O4: 822.4402; found, 822.4405.

ph-TDI: 1H NMR (400 MHz, CDCl3, 298K): δ = 8.50-8.48 (sd, J = 7.6 Hz, 4H), 7.45-7.39 (m, 16H), 7.37-7.34 (m, 8H), 5.23-5.16 (m, 2H), 2.31-2.22 (m, 4H), 1.85-1.79 (m, 4H), 1.30-1.25 (m, 24H), 0.84-0.81 (m, 12H); 13C NMR (100 MHz, CDCl3, 298K): δ = 165.04, 163.99, 143.39, 140.20, 135.72, 135.08, 133.80, 129.87, 129.43, 128.81, 127.92, 127.35, 121.29, 120.64, 54.53, 32.36, 31.76, 26.59, 22.56, 14.03; HRMS (MALDI, 100%): calcd (%) for C80H74N2O4: 1126.5654; found, 1126.5655.

th-TDI: 1H NMR (500 MHz, CDCl2CDCl2, 373K): δ = 8.55 (s, 4H), 7.76 (s, 4H), 7.41-7.40 (d, J = 5.0 Hz, 4H), 7.19 (s, 4H), 7.13-7.11 (m, 4H), 5.18-5.13 (m, 2H), 2.26-2.22 (m, 4H), 1.90-1.86 (m, 4H), 1.39-1.31 (m, 24H), 0.88-0.85 (m, 12H); 13C NMR (125 MHz, CDCl2CDCl2, 373K): δ = 164.02, 144.85, 135.82, 135.14, 132.76, 129.49, 129.44, 129.17, 129.07, 128.50, 128.02, 127.47, 126.96, 121.33, 54.90, 32.56, 31.72, 26.63, 22.45, 13.88; HRMS (MALDI, 100%): calcd (%) for C72H66N2O4S4: 1150.3910; found, 1150.3917.

2. Characterization of TDI, ph-TDI and th-TDI

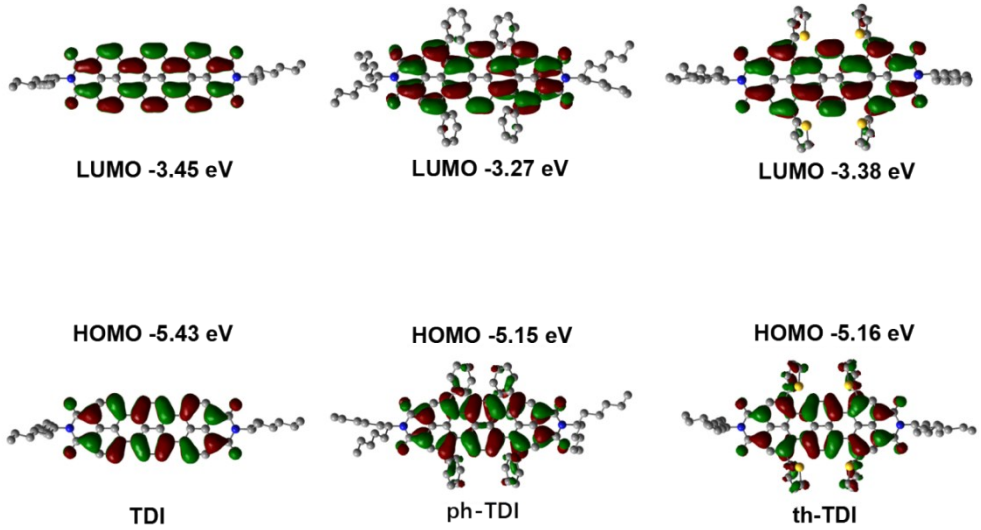

Figure S1. Energies and shapes of B3LYP/6-31G (d,p) frontier π orbitals of model TDI, ph-TDI and th-TDI.

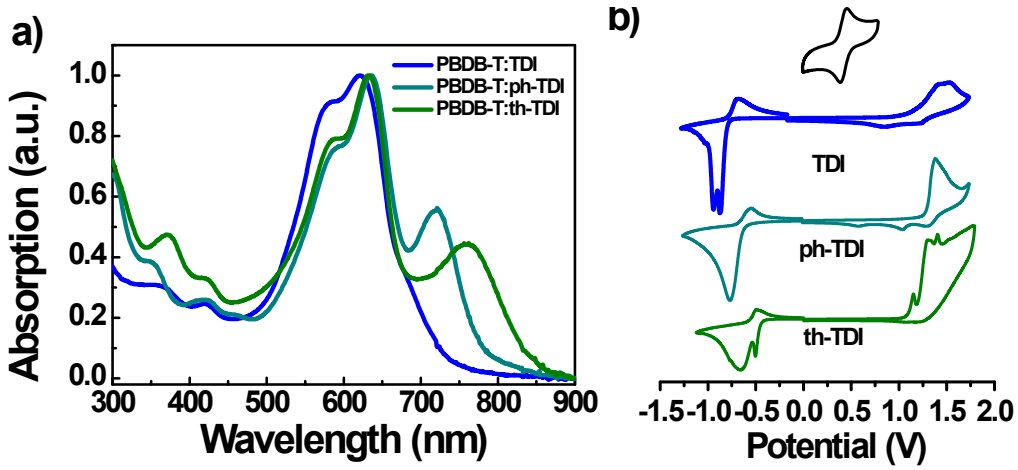

Figure S2. a) UV-vis normalized absorption spectra of TDI, ph-TDI and th-TDI blend films and b) CV plots of TDI, ph-TDI and th-TDI in film.

3. Devices Fabrication and Characterization.

OFET devices: The organic field-effect transistors were fabricated on a commercial $Si/SiO_2/Au$ substrate purchased from First MEMS Co. Ltd. A heavily N-doped Si wafer with a SiO_2 layer of 300 nm served as the gate electrode and dielectric layer, respectively. The source-drain electrodes of Ti (2 nm)/Au (28 nm) were sputtered and patterned by a lift-off technique. The gate dielectrics were treated with octadecyltrichlorosilane (ODTS) in a vacuum oven at 120 ℃. The treated substrates were treated with hexane, chloroform and isopropyl alcohol. Before spin-coating the solution of TDIs, the sample was dissolved into the chloroform with 10% n-hexane. Then the solution was spin-coated onto the substrates with the thickness of 30-50 nm and thermally annealed at 200 ℃ for 10 min in a glovebox filled with N_2. The mobilities were calculated from the saturation region with the following equation: $I_{DS}=(W/2L)C_i\mu(V_G-V_T)^2$, where I_{DS} is the drain-source current, W is the channel width (1400 μm), L is the channel length (50 μm), μ is the field-effect mobility, C_i is the capacitance per unit area of the gate dielectric layer, V_G and V_T are the gate voltage and threshold voltage, respectively.

Table S1. The p-channel and n-channel characteristics of ambipolar OFETs based on TDI, ph-TDI and th-TDI with V_{SD} = 100 V and -100 V.

Sample	Mobility ($cm^2\ V^{-1}\ s^{-1}$)		V_T (V)	I_{on}/I_{off}
TDI	μ_h	1.5×10^{-4}	-43.5	1×10^{1}
	μ_e	7.3×10^{-3}	15.5	1×10^{3}
ph-TDI	μ_h	2.3×10^{-2}	-57.3	4×10^{1}
	μ_e	2.8×10^{-2}	9.3	2×10^{2}
Th-TDI	μ_h	5.5×10^{-3}	-54.0	1×10^{1}
	μ_e	1.2×10^{-2}	5.0	1×10^{2}

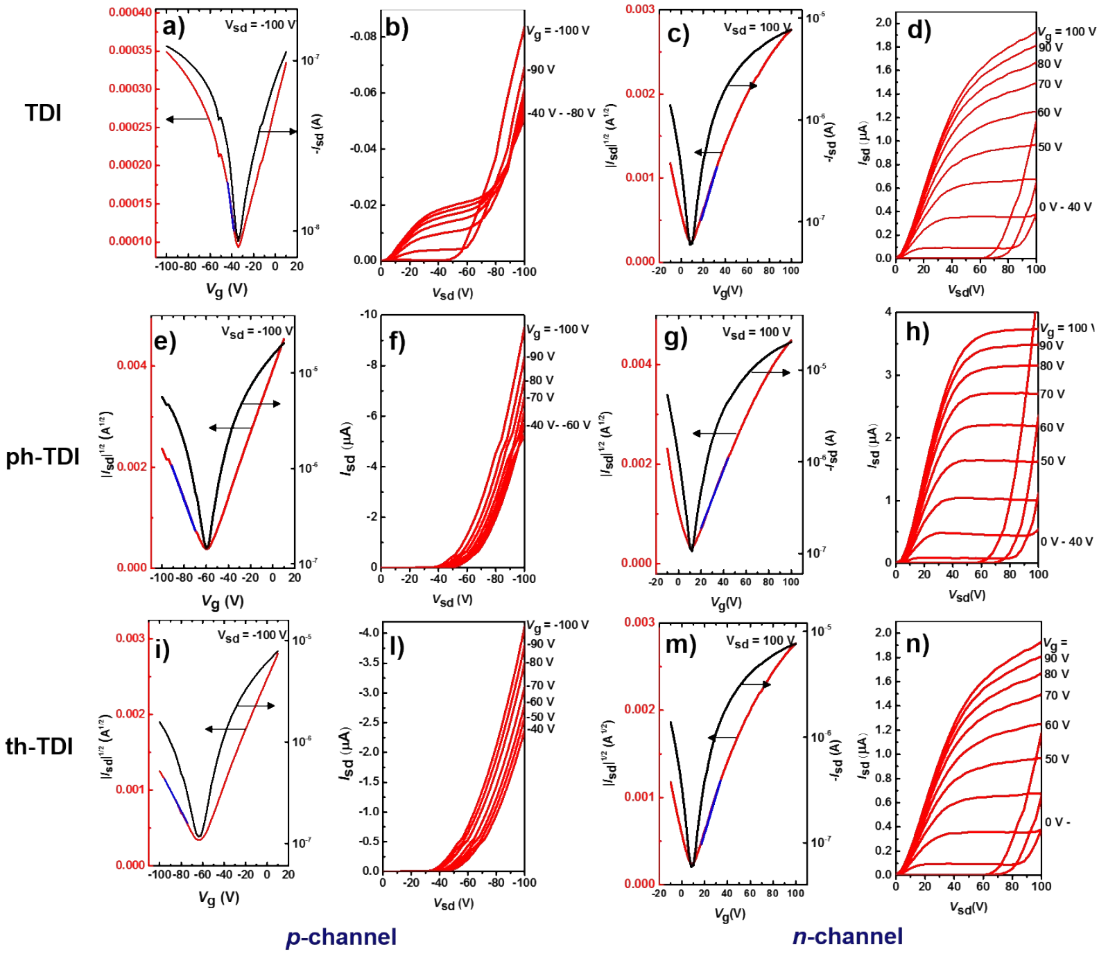

Figure S3. Current-voltage *(J-V)* characteristics of OFETs based on TDI, ph-TDI and th-TDI with optimized thin-film fabricated by CF+10% *n*-Hexane annealed at 200 ℃. (a), (e), (i) Transfer characteristics of *p*-channel for films with V_{SD}=-100 V; (c), (g), (m) Transfer characteristics of *n*-channel for films with V_{SD}=100 V; (b), (f), (l) Output characteristics of *p*-channel for films; (d), (h), (n) Output characteristics of *n*-channel for films (L=1400 μm and W= 50 μm)

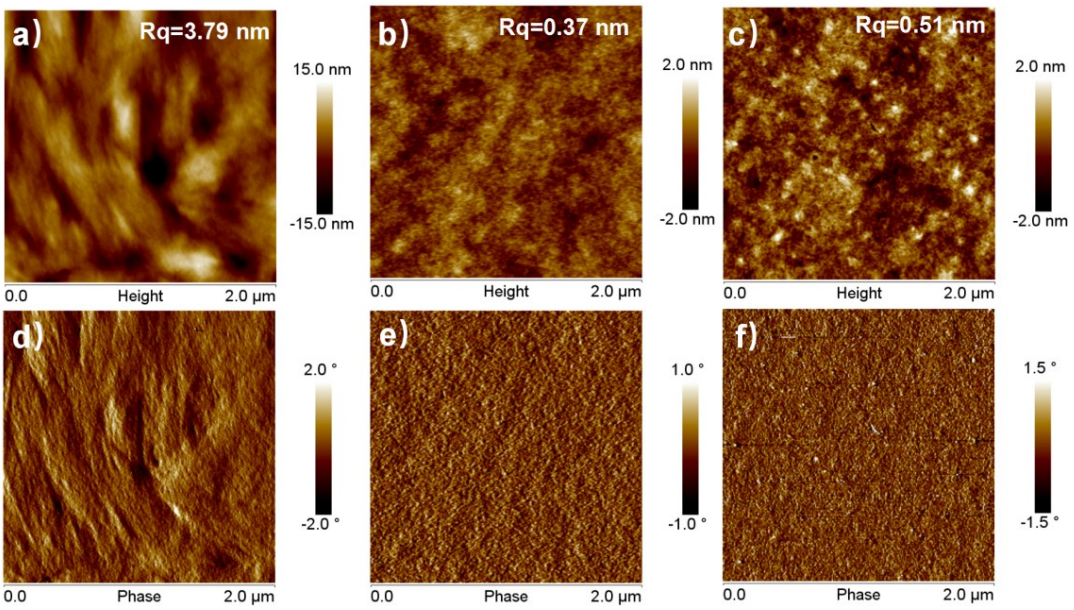

Figure S4. a-c) AFM height images, d-f) AFM phase images of TDI film, ph-TDI film and th-TDI film, respectively.

Photovoltaic devices: In an ultrasonic bath, the ITO-coated glass (15 Ω/□) was cleaned with deionized water, acetone, and isopropanol, respectively. After oxygen plasma cleaning for 20 min, a 40 nm thick ZnO cathode buffer layer was spin-cast onto the ITO substrate and then dried by baking in an oven at 200 °C for 60 min. Of which, the polymeric donor PBDB-T (M_n=22923 g/mol, M_w=54445 g/mol, D=2.375) was selected as the donor material. The active layer were then deposited on top of the ZnO layer by spin-coating from CB or *o*-xylene solution (8 mg/mL of polymers) of PBDB-T:acceptor and different concentration of 1-CN as a processing additive was added to the solutions before use. The active layers solution using CB as the host solvent was stirred at the room temperature and the solution in *o*-xylene was stirred at 70 °C for at least 8 hours. Then, the active layer solution was spin-coated onto the ZnO buffer layer at the speed of 2000 rpm for 80-nm-thick active layers. Then the device fabrication process was completed by thermally evaporating 10-nm-thick MoO_3 as the anode buffer layer under vacuum at a pressure of 3×10^{-4} Pa. Finally, 100-nm-thick Al layer was evaporated on top of the active layer. The overlapping area between the cathode and anode defined a pixel size of 0.04 cm^2. The *J*−*V* measurement was performed via the solar simulator (SS-F5-3A, Enlitech) along with AM 1.5G spectra whose intensity was calibrated by the certified standard silicon solar cell (SRC-2020, Enlitech) at 100 mw/cm^2. The EQE data were obtained using a solar cell spectral

response measurement system (QE-R3011, Enli Technology Co. Ltd). The film thickness data were obtained employing a surface profilometer (Dektak XT, Bruker).

Table S2. Photovoltaic parameters of the cells using CB as the host solvent under AM 1.5G illumination of 100 mW/cm^2

Blend	Ratio(w/w)	Solvent	V_{OC} (V)	J_{SC} (mA cm^{-2})	FF	PCE(%)
PBDB-T:TDI	1.5:1	w/o	0.747	3.36	0.37	0.93
	1:1	w/o	0.750	4.93	0.44	1.62
	1:1	1% CN	0.726	2.03	0.33	0.49
	1:1.5	w/o	0.745	4.65	0.44	1.52
PBDB-T:ph-TDI	1:1	w/o	0.923	8.91	0.41	3.36
	1:1	0.5% CN	0.930	9.78	0.48	4.40
	1:1	1% CN	0.934	9.64	0.49	4.43
	1:1	2% CN	0.930	9.73	0.48	4.23
PBDB-T:th-TDI	1:1	w/o	0.825	9.01	0.42	3.15
	1:1	1% CN	0.823	9.13	0.47	3.50

Table S3. Photovoltaic parameters of the cells using o-xylene as the host solvent under AM 1.5G illumination of 100 mW/cm^2

Blend	Solvent	V_{OC} (V)	J_{SC} (mA cm^{-2})	FF	PCE (%)
PBDB-T:TDI	w/o	0.735	4.41	0.35	1.13
	3% CN	0.787	4.14	0.44	1.44
PBDB-T:ph-TDI	w/o	0.892	8.11	0.38	2.74
	1% CN	0.912	9.70	0.45	4.00
	2% CN	0.925	9.79	0.51	4.64
	3% CN	0.938	11.10	0.49	5.10
	4% CN	0.930	9.04	0.51	4.33
PBDB-T:th-TDI	w/o	0.789	8.11	0.39	2.47
	1% CN	0.811	9.58	0.46	3.55
	2% CN	0.817	9.95	0.49	3.96
	3% CN	0.840	10.46	0.47	4.12
	4% CN	0.828	9.23	0.50	3.86

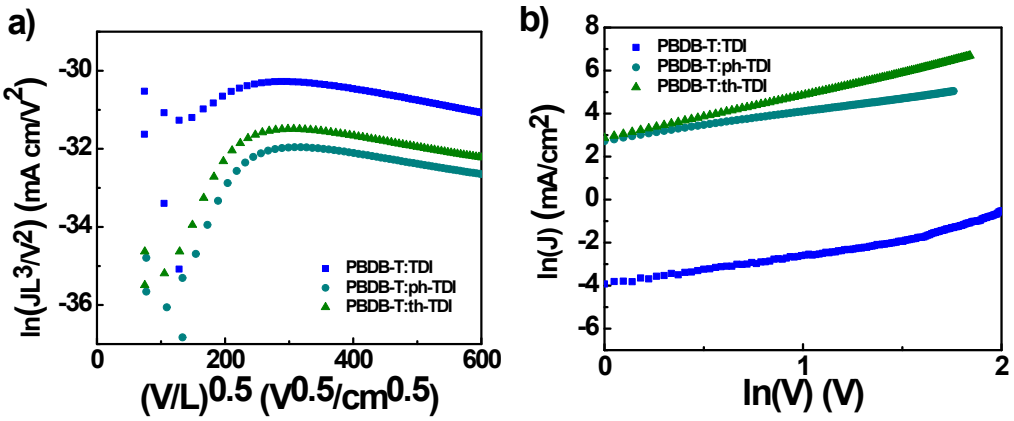

Figure S5. a) Plots of $\ln(JL^3/V^2)$ VS $\ln(V/L)^{0.5}$ obtained from the hole-only devices and b) plots of lnJ vs lnV obtained from the electron-only devices for the optimized solar cells based on PBDB-T:TDI, PBDB-T:ph-TDI and PBDB-T:th-TDI active layers.

Table S4. Hole and electron mobilities of TDI, ph-TDI and th-TDI blend films processed by *o*-xylene and 1-CN solvent.

Blend	Hole mobility ($cm^2/(V\ s)$)	Electron mobility ($cm^2/(V\ s)$)	μ_h/μ_e
PBDB-T:TDI	$6.93*10^{-4}$	$3.97*10^{-8}$	17204
PBDB-T:ph-TDI	$1.27*10^{-4}$	$2.48*10^{-5}$	5.12
PBDB-T:th-TDI	$2.02*10^{-4}$	$3.29*10^{-5}$	6.14

4. ^{1}H NMR, ^{13}C NMR and HRMS Spectra

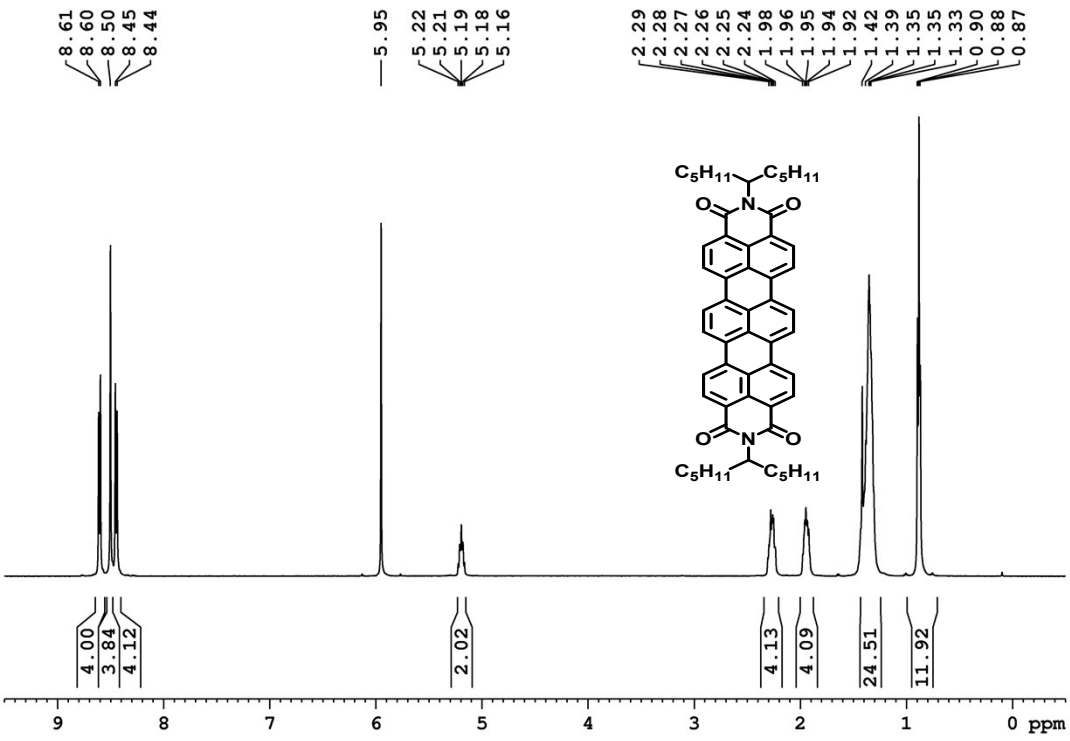

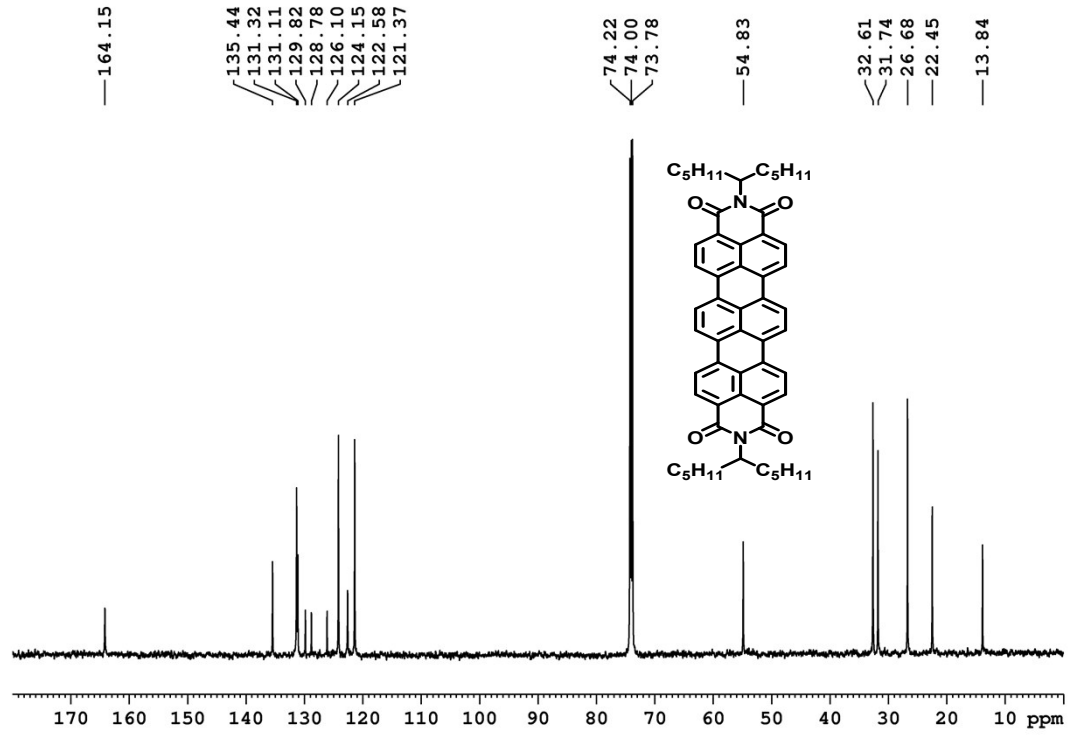

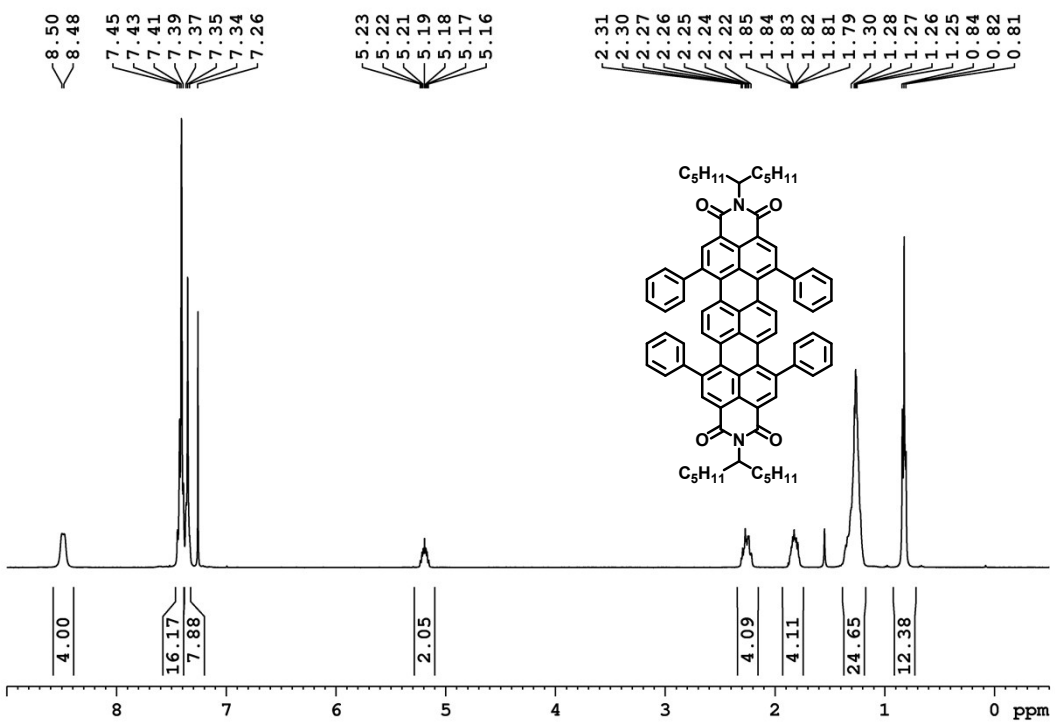
8.50
8.48
7.45
7.43
7.41
7.39
7.37
7.35
7.34
7.26
5.23
5.22
5.21
5.19
5.18
5.17
5.16
2.31
2.30
2.27
2.26
2.25
2.24
2.22
1.85
1.84
1.83
1.82
1.81
1.79
1.30
1.28
1.27
1.26
1.25
0.84
0.82
0.81
4.00
16.17
7.88
2.05
4.09
4.11
24.65
12.38
8
7
6
5
4
3
2
1
0 ppm

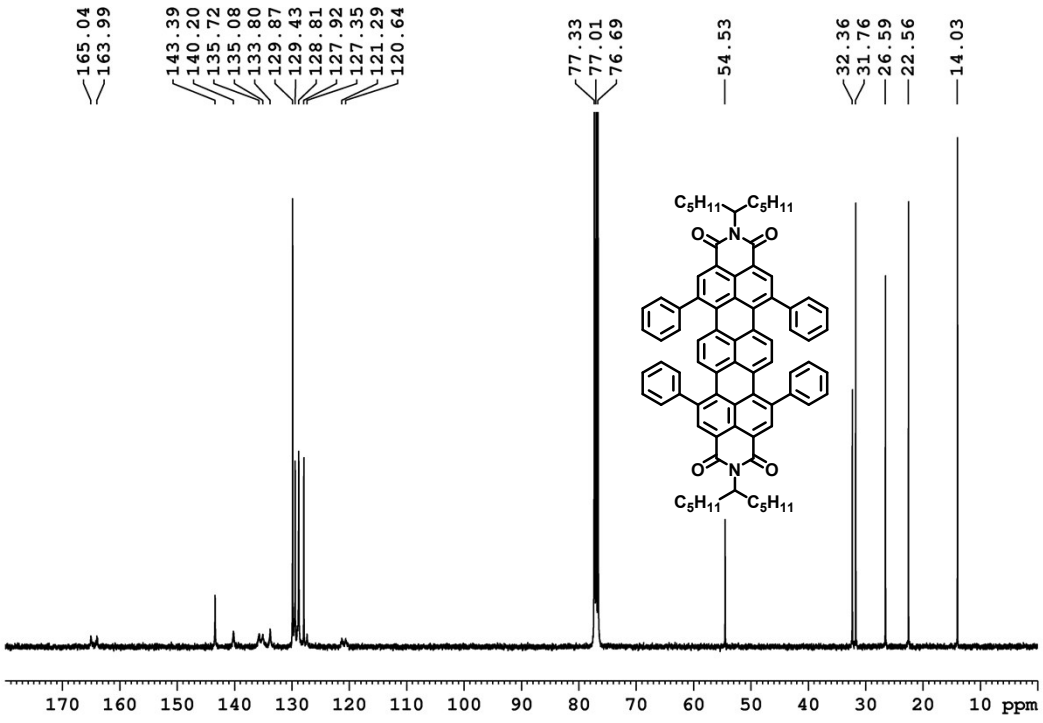
165.04
163.99
143.39
140.20
135.72
135.08
133.80
129.87
129.43
128.81
127.92
127.35
121.29
120.64
77.33
77.01
76.69
54.53
32.36
31.76
26.59
22.56
14.03
170
160
150
140
130
120
110
100
90
80
70
60
50
40
30
20
10 ppm